Advances in Concrete Construction, *Vol. 7, No. 3 (2019) 151-166*
DOI: https://doi.org/10.12989/acc.2019.7.3.151

Improved analytical method for adhesive stresses in plated beam: Effect of shear deformation

B. Guenaneche[*1], S. Benyoucef[1], A. Tounsi[1,2] and E.A. Adda Bedia[3]

[1]*Civil Engineering Department, Faculty of Technology, Material and Hydrology Laboratory, University of Sidi Bel Abbes, Algeria*
[2]*Department of Civil and Environmental Engineering, King Fahd University of Petroleum & Minerals, 31261 Dhahran, Eastern Province, Saudi Arabia*
[3]*Centre of Excellence for Advanced Materials Research, King Abdulaziz University, Jeddah, 21589, Saudi Arabia*

(Received July 4, 2018, Revised February 20, 2019, Accepted February 24, 2019)

Abstract. This paper introduces a new efficient analytical method, based on shear deformations obtained with 2D elasticity theory approach, to perform an explicit closed-form solution for calculation the interfacial shear and normal stresses in plated RC beam. The materials of plate, necessary for the reinforcement of the beam, are in general made with fiber reinforced polymers (Carbon or Glass) or steel. The experimental tests showed that at the ends of the plate, high shear and normal stresses are developed, consequently a debonding phenomenon at this position produce a sudden failure of the soffit plate. The interfacial stresses play a significant role in understanding this premature debonding failure of such repaired structures. In order to efficiently model the calculation of the interfacial stresses we have integrated the effect of shear deformations using the equilibrium equations of the elasticity. The approach of this method includes stress-strain and strain-displacement relationships for the adhesive and adherends. The use of the stresses continuity conditions at interfaces between the adhesive and adherents, results pair of second-order and fourth-order coupled ordinary differential equations. The analytical solution for this coupled differential equations give new explicit closed-form solution including shear deformations effects. This new solution is indented for applications of all plated beam. Finally, numerical results obtained with this method are in agreement of the existing solutions and the experimental results.

Keywords: two-dimensional elasticity; RC beam; interfacial shear stress; interfacial normal stress; debonding; coupled differential equations; soffit plate; shear deformations

1. Introduction

During the last decade, the reinforcement of concrete and steel beams by bonding a soffit plate fabricated by either steel or fibre-reinforced plastics (FRP) has been the subject of much research and demonstrated to be a highly effective renovation method in civil and structural engineering because of its benefits such as significantly improving the rigidity and strength of an existing structural element with reduced impact on the surrounding environment (Hollaway and Leeming 1999, Kreja 2011, Panjehpour *et al*. 2014a, b, Ahmed 2014, Akavci and Tanrikulu 2015, Mahi *et al*. 2015, Draiche *et al*. 2016, Chikh *et al*. 2017, Aldousari 2017, Sahoo *et al*. 2017, Zine *et al*. 2018, Kaci *et al*. 2018). It is largely remarked that in such a redeveloped beam, one of the important modes of failure is the plate end delaminating of the soffit plate from concrete beam, which depends widely on the adhesive shear and normal stress concentration at the cut-off points of the plate (Teng *et al*. 2002a). Many investigations have been carried out, either numerically, analytically or both, to computed the adhesive stresses (Vilnay 1988, Roberts 1989, Roberts and Haji-Kazemi 1989, Taljsten 1997, Malek *et al*. 1998, Etman and Beeby 2000, Maalej and Bian 2001, Ye 2001, Shen *et al*. 2001, Teng *et al*. 2002b, Teng *et al*. 2003, Yang *et al*. 2004, Maalej and Leong 2005, Wu *et al*. 2005, Tounsi *et al*. 2009, Rabahi *et al*. 2015, Daouadji *et al*. 2016, Bensaid and Kerboua 2017, Daouadji 2017). However, most of these studies did not simultaneously include the influences of axial, bending and shear deformations in the bonded plate and the concrete beam, which may conduct to results with insufficient precision in some cases. Adhesive stress investigations considering the impact of shear deformation are rare. In some articles, coupled differential equations have been changed to decoupled equations, and the obtained solutions are insufficiently accurate. Although Smith and Teng (2001), Yang and Wu (2007) introduced and solved the dominant differential equations, the first article neglected the influence of shear strain to determine decoupled equations, and the second one portioned the differential equations in two parts (with and without the effect of shear deformation) and employed the Fourier series to increase shear deformation. The superposition and the Galerkin method were employed to determine the solutions to the differential equations (Yang and Wu 2007). A significant number of high-order analytical methods exist to obtain the adhesive shear and normal stresses (Rabinovitch and Frostig 2000, Shen *et al*. 2001). It should

*Corresponding author, Ph.D.
E-mail: guenanecheb@yahoo.fr

ISSN: 2287-5301 (Print), 2287-531X (Online)

be also indicated that the method of Rabinovitch and Frostig (2000) does not give explicit expressions for the adhesive stresses. In this method the constants of integration are not provided and only the boundary conditions are presented. It thus seems impossible to determine results to propose a design rule (Smith and Teng 2001, Shen *et al*. 2001). The accuracy of this investigation has also been checked (Shen *et al*. 2001, Smith and Teng 2001). In another high-level analysis introduced by Shen *et al*. (2001), other explicit relations were obtained but the expressions do not take into account the influences of shear curvature and shear deformation in the composite beam. It is well known that Timoshenko's theory is a refined beam theory that considers shear deformation effect (Antes 2003).

In this paper, an efficient model is developed to calculate the interfacial stresses in bonded beam by introducing the shear deformation using the equilibrium equations of the elasticity. It is believed that the proposed formulation will be of interest to civil and structural engineers and researchers.

2. Mathematical formulation

2.1 Assumptions

The beam and the soffit plate are denoted respectively adherents 1 and 2. The assumptions adopted in present solution are summarized below.

- Linear elastic behaviour of adherends 1, 2 and adhesive layer is assumed.
- The interfacial stresses are invariant across its thickness of adhesive layer.
- The curvatures of the RC beam and soffit plate are assumed to be the same.
- The effects of bending deformations are neglected in adhesive layer.

Perfect bonding between the RC beam, the FRP strip, and the adhesive and the adhesive layer is assumed.
It is important to declare that in present paper the interfacial stress is under consideration only at the middle of adhesive thickness

2.2 Equilibrium and compatibility equations

By referring to Fig. 1 and Fig. 2, the global equilibrium equations for the two adherents can be obtained as follows

$$\frac{dN_i(x)}{dx} = (-1)^i \cdot b_i \cdot \tau(x) \quad \text{i} = 1,2 \tag{1}$$

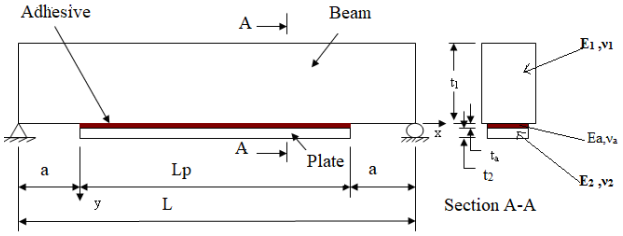

Fig. 1 Schematic configuration of plated beam: geometrical and material parameters

$$\frac{dV_i(x)}{dx} = (-1)^i \cdot b_i \cdot \sigma(x) \quad \text{i} = 1,2 \tag{2}$$

$$\frac{dM_i(x)}{dx} = V_i(x) - b_i \cdot \tau(x) \cdot \frac{t_i}{2} \quad i = 1,2 \tag{3}$$

The longitudinal normal stresses, $\sigma_i(x,y)\ i = 1,2$ are assumed to vary linearly with transverse coordinates y_i.

$$\sigma_i(x,y) = \frac{N_i(x)}{b_i \cdot t_i} - \frac{6 \cdot M_i(x)}{b_1 \cdot t_i^2} \cdot \left(1 - \frac{2 \cdot y}{t_i}\right) i = 1,2 \tag{4}$$

Where $0 \le y \le t_i$

From the two-dimensional elasticity theory, these stress components defined by Alfredsson and Höberg (2008) should satisfy the following equations of equilibrium.

$$\frac{\partial \sigma_{ix}}{\partial x} + \frac{\partial \tau_i}{\partial y} = 0 \quad \text{i} = 1,2 \tag{5}$$

Substituting Eq. (4) into Eq. (5) and using Eqs. (1), (3), (4), after integrating and using the Eq. (6) of shear stress continuity conditions at the beam-plate interface and the conditions of zero shear stress on the top and bottom surfaces respectively of the beam and the plate

$$\begin{gathered}(\tau_1(x, y = 0) = 0 \ \text{, and} \\ \tau_2(x, y = t_2) = 0 \\ \tau_1(x, y = t_1) = \tau_2(x, y = 0)) = \tau(x)\end{gathered} \tag{6}$$

The shear stresses are given by the following equations

$$\begin{aligned}\tau_1(x,y) &= (-\frac{2 \cdot y}{t_1} + \frac{3 \cdot y^2}{t_1^2}) \cdot \tau(x) \\ &+ V_1(x) \cdot \frac{6}{b_1 \cdot t_1^2} \cdot (y - \frac{y^2}{t_1})\end{aligned} \tag{7a}$$

$$\begin{aligned}\tau_2(x,y) &= (1 - \frac{4 \cdot y}{t_2} + \frac{3 \cdot y^2}{t_2^2}) \cdot \tau(x) \\ &+ V_2(x) \cdot \frac{6}{b_2 \cdot t_2^2} \cdot (y - \frac{y^2}{t_2})\end{aligned} \tag{7b}$$

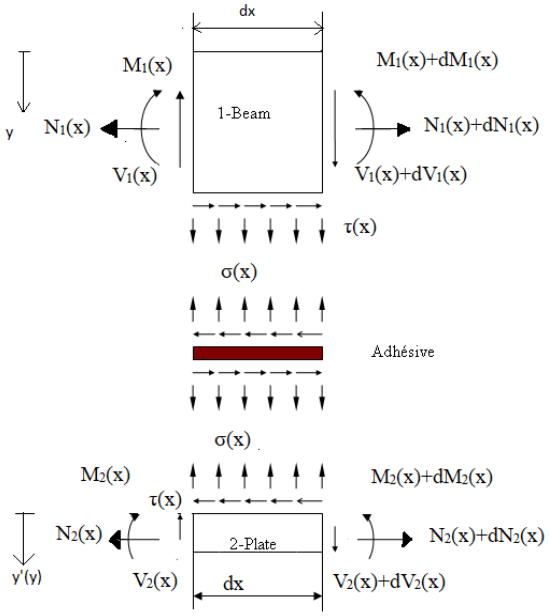

Fig. 2 Free-body stress equilibrium diagram

The shear stresses, thus obtained, are shape parabolic through thickness of the adherend

2.3 Stress-strain and strain-displacements equations

Shear stresses determined by the Eqs. (7a) and (7b) can be expressed as a function of shear strain by the following relationship.

$$\gamma_i(x,y) = \frac{\tau_i(x,y)}{G_i} \quad i = 1,2 \tag{8}$$

With G_i is the transverse shear modulus of the adherend *i*.

Shear strain $\gamma_i(x,y)$ is expressed in terms of horizontal and vertical displacements functions $U_i^N(x,y)$ and $V_i^N(x,y)$ by the following relationship.

$$\gamma_i(x,y) = \frac{\partial U_i^N(x,y)}{\partial y} + \frac{\partial V_i^N(x,y)}{\partial x} \quad i = 1,2 \tag{9}$$

Neglecting the variations of transverse displacement $\frac{\partial V_i^N(x,y)}{\partial x}$, induced by the longitudinal forces with the longitudinal coordinate *x*, the shear deformation is expressed by the following equation.

$$\gamma_i(x,y) \approx \frac{\partial U_i^N(x,y)}{\partial y} \quad i = 1,2 \tag{10}$$

The longitudinal displacement functions $U_1^N(x,y)$ for the beam an $U_2^N(x,y)$ for the plate, due to then longitudinal forces, are determined using Eqs. (8) and (10). The longitudinal displacements $U_i^N(x,y)$ of the two adherents (Tsai 1998, Tounsi 2006) are given by the following equation.

$$U_i^N(x,y) = \int_0^y \frac{\tau_i(x,y)}{G_i} \cdot dy + U_i^N(x,y=0) \tag{11}$$

By substituting Eq. (6) in Eq. (11) and after integration, we obtain the following expression of the longitudinal displacements.

$$U_1^N(x,y) = \left(-\frac{y^2}{t_1} + \frac{y^3}{t_1^2}\right) \cdot \frac{\tau(x)}{G_1} + \frac{V_1(x)}{G_1} \cdot \frac{6}{b_1 \cdot t_1^2} \cdot \left(\frac{y^2}{2} - \frac{y^3}{3 \cdot t_1}\right) + U_1^N(x,y=0) \tag{12a}$$

$$U_2^N(x,y) = U_2^N(x,y=0) + (y - \frac{2 \cdot y^2}{t_2} + \frac{y^3}{t_2^2}) \cdot \frac{\tau(x)}{G_2} + \frac{V_2(x)}{G_2} \cdot \frac{6}{b_2 \cdot t_2^2} \cdot (\frac{y^2}{2} - \frac{y^3}{3 \cdot t_2}) \tag{12b}$$

The adhesive layer is subjected in its upper and lower edges to longitudinal displacements ($u_1^N(x,y)$ and $u_2^N(x,y)$) generated by the beam (adherent 1) and the plate (adherent 2). These displacements are obtained by checking the following boundary conditions.

$$u_1^N(x,y) = U_1^N(x,y=t_1) \;\&$$

$$u_2^N(x,y) = U_2^N(x,y=0) \tag{13}$$

Thus the longitudinal displacements $U_1^N(x,y)$ and $U_2^N(x,y)$ based to $u_1^N(x,y)$ and$u_2^N(x,y)$ respectively are given by the following equations.

$$U_1^N(x,y) = u_1^N(x) + (-\frac{y^2}{t_1} + \frac{y^3}{t_1^2}) \cdot \frac{\tau(x)}{G_1} - \frac{V_1(x)}{G_1 \cdot b_1} \cdot (1 - \frac{3 \cdot y^2}{t_1^2} + \frac{2 \cdot y^3}{t_1^3}) \tag{14a}$$

$$U_2^N(x,y) = u_2^N(x) + (y - \frac{2 \cdot y^2}{t_2} + \frac{y^3}{t_2^2}) \cdot \frac{\tau(x)}{G_2} + \frac{V_2(x)}{G_2 \cdot b_2} \cdot (\frac{3 \cdot y^2}{t_2^2} - \frac{2 \cdot y^3}{t_2^3}) \tag{14b}$$

The longitudinal resultant forces, N_1 and N_2, for the upper and lower adherends, respectively, are

$$N_1 = b_1 \cdot \int_0^{t_1} \sigma_1^N(x,y)\, dy \tag{15a}$$

$$N_2 = b_2 \cdot \int_0^{t_2} \sigma_2^N(x,y)\, dy \tag{15b}$$

Where $\sigma_i(x,y)\; i = 1,2$ are longitudinal normal stresses for the upper and lower adherends, respectively. By changing these stresses into functions of displacements and substituting Eqs. (14a) and (14b) into the displacements, Eqs. (15a) and (15b) can be rewritten as

$$N_1 = E_1 \cdot b_1 \cdot \int_0^{t_1} \frac{dU_1^N(x,y)}{dx} dy = E_1 \cdot A_1 \cdot \left(\frac{du_1^N}{dx} - \frac{t_1}{12 \cdot G_1} \cdot \frac{d\tau(x)}{dx} - \frac{y_1}{G_1 \cdot A_1} \cdot \frac{dV_1(x)}{dx} \right) \tag{16a}$$

And

$$N_2 = E_2 \cdot b_2 \cdot \int_0^{t_2} \frac{dU_2^N(x,y)}{dx} dy = E_2 \cdot A_2 \cdot \left(\frac{du_2^N}{dx} - \frac{t_2}{12 \cdot G_2} \cdot \frac{d\tau(x)}{dx} - \frac{y_2}{G_2 \cdot A_2} \cdot \frac{dV_2(x)}{dx} \right) \tag{16b}$$

Where $A_i = b_i \cdot t_i$ and $y_i = \frac{t_i}{2}$, $i = 1,2$

The strains in the RC beam near the adhesive interface and the external FRP reinforcement can be expressed, as

$$\varepsilon_i(x) = \frac{du_i(x)}{dx} = \varepsilon_i^M(x) + \varepsilon_i^N(x) \quad i = 1,2 \tag{17}$$

Where and $u_1^N(x,y)$ are the longitudinal displacements

at the bottom of adherend1 and $u_2^N(x,y)$ the top of adherend2, respectively. The strains induced by the bending moment at adherends $\varepsilon_i^N(x)\ i=1,2$ are written as follows

$$\varepsilon_i^M(x) = \pm\frac{y_i}{E_i \cdot I_i}\cdot M_i(x) \quad i=1,2 \tag{18}$$

Where E_i is the elastic modulus and I_i the second moment of area.

$M_i(x)$ is the bending moment while y_1 and y_2 are the distances from the bottom of beam and the top of plate to their respective centroid.

$\varepsilon_i^N(x)\ i=1,2$ are the unknown longitudinal strains of the RC beam and FRP reinforcement, respectively, at the adhesive interface and they are due to the longitudinal forces. These strains are given as follows

$$\varepsilon_i^N(x) = \frac{du_i^N(x)}{dx} \quad i=1,2 \tag{19}$$

Hence, the longitudinal strains induced by the longitudinal forces (Eq. (19)) can be expressed as

$$\varepsilon_i^N(x) = \frac{du_i^N(x)}{dx} = \frac{N_i}{E_i \cdot I_i} \pm \frac{t_i}{12\cdot G_i}\cdot\frac{d\tau(x)}{dx} \pm \frac{y_i}{G_i \cdot A_i}\cdot\frac{dV_i(x)}{dx} \quad i=1,2 \tag{20}$$

The total strains equations for the adherend i are given as follows

$$\varepsilon_i(x) = \pm\cdot\frac{y_i}{E_i \cdot I_i}\cdot M_i(x) + \frac{N_i}{E_i \cdot I_i} \pm \frac{t_i}{12\cdot G_i}\cdot\frac{d\tau(x)}{dx} \pm \frac{y_i}{G_i \cdot A_i}\cdot\frac{dV_i(x)}{dx} \quad i=1,2 \tag{21}$$

2.4 Governing differential equations for interfacial stresses between an RC beam and soffit plate

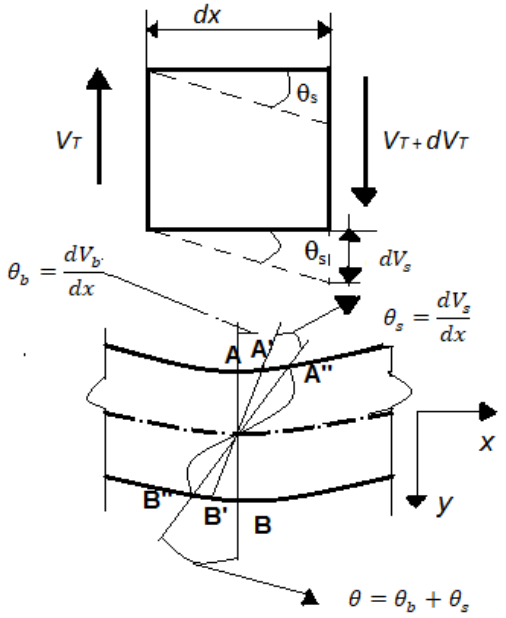

Fig. 3 Bending and shear curvatures in Timoshenko composite beam

2.4.1 Interfacial shear stress

The shear strain γ in the adhesive layer may be represented by Eq. (9)

$$\gamma(x,y) = \frac{du(x,y)}{dy} + \frac{dv(x,y)}{dx} \tag{22}$$

With $u_1(x,y) = U_1^N(x,y=t_1)$, $u_2(x,y) = U_2^N(x,y=0)$ and $v(x,y) \approx V_i^N(x,y)$.

The interfacial shear stress $\tau(x)$, which is related to the shear strain γ expressed by Smith and Teng (2001), are derived from Eq. (22)

$$\tau(x) = G_a\cdot\gamma = G_a\cdot\left(\frac{du(x,y)}{dy} + \frac{dv(x,y)}{dx}\right) \tag{23}$$

Where G_a is shear modulus of adhesive layer. The first derivative of $\tau(x)$ with respect to x is as follow

$$\frac{d\tau(x)}{dx} = G_a\cdot\left(\frac{d^2u(x,y)}{dx\,dy} + \frac{d^2v(x,y)}{dx^2}\right) \tag{24}$$

The second derivative of $v(x,y)$ with respect to x defines the total curvature of the Timoshenko composite beam at a distance x. This total curvature of the plated beam $\frac{d\theta}{dx}$ is the sum of the bending curvature $\frac{d\theta_b}{dx}$ and shear curvature $\frac{d\theta_s}{dx}$ defined by Edalati and Fereidon (2012). These curvatures may be written as follows

$$\begin{cases} \dfrac{d\theta_b}{dx} = \dfrac{d^2v_b(x,y)}{dx^2} = \dfrac{-M_T(x)}{(EI)_t} \\ \dfrac{d\theta_s}{dx} = \dfrac{d^2v_s(x,y)}{dx^2} = \dfrac{-1}{(\alpha GA)_t}\cdot\dfrac{dV_T(x)}{dx} \\ \dfrac{d\theta}{dx} = \dfrac{d^2v(x,y)}{dx^2} = \dfrac{d\theta_b}{dx} + \dfrac{d\theta_s}{dx} \end{cases} \tag{25}$$

In which $V_b(x,y)$,$V_s(x,y)$ are transversal displacement respectively at the bending, at the shear. $V(x,y)$ is total transversal displacement in a cross-section of the composite beam. $V_T(x)$ and $M_T(x)$=total shear force and the total bending moment in the composite section, respectively; $(\alpha\cdot GA)_t$ and $(EI)_t$ effective shear rigidity and effective flexural rigidity in the total composite section, which may be obtained by Timoshenko and Gere (1984) and Stafford and Coull (1991)

$$\begin{cases} (\alpha GA)_t = \alpha(G_1A_1 + G_2A_2) \\ (EI)_t = (E_1I_1 + E_2I_2) \\ I_1 = \dfrac{I_{1b}}{1+r_{1e}} \\ I_2 = \dfrac{I_{2b}}{1+r_{2e}} \end{cases} \tag{26}$$

In which

E_i , I_i , G_i and A_i are modulus of elasticity, the reduced effective moment of inertia with respect to the centroid. The moments of inertia in RC beam and the soffit plate

I_b are defined by Stafford and Coull (1991). The parameters $r_{ie}\ i=1,2$ of the two adherents are given by Edalati and Fereidon (2012) from the following relationships

$$\begin{cases} r_{1e} = \dfrac{48 \cdot E_1 \cdot I_{1b}}{5 \cdot \alpha \cdot G_1 \cdot A_1 \cdot L^2} \\ r_{2e} = \dfrac{48 \cdot E_2 \cdot I_{2b}}{5 \cdot \alpha \cdot G_2 \cdot A_2 \cdot L_p^2} \end{cases} \quad (27)$$

In which α is shape factor for the shear stresses expressed by Cowper (1966) and given with following relationship for solid rectangular

$$\alpha = \frac{10 \cdot (1+\nu)}{12 + 11 \cdot \nu} \quad (28)$$

The coefficient ν is Poisson's ratio.

Finally, the total curvature of a differential element in plated beam Timoshenko may be expressed as follows

$$\frac{d^2v(x,y)}{dx^2} = \frac{d\theta_b}{dx} + \frac{d\theta_s}{dx} = \frac{-M_T(x)}{(EI)_t} + \frac{-1}{(\alpha \cdot GA)_t} \cdot \frac{dV_T(x)}{dx} \quad (29)$$

The adhesive layer is assumed to be subjected to uniform shear stresses and therefore $u(x,y)$ must vary linearly across the adhesive thickness ta, so first derivative of the displacement$u(x,y)$ can be obtained by following relationship

$$\frac{du(x,y)}{dy} = \frac{1}{t_a} \cdot [u_2(x) - u_1(x)] \quad (30)$$

The second derivative of Eq. (30) with respect to *x* is

$$\frac{d^2u(x,y)}{dx\,dy} = \frac{1}{t_a} \cdot \left[\frac{du_2(x)}{dx} - \frac{du_1(x)}{dx}\right] \quad (31)$$

Where $u_1(x)$ and $u_2(x)$ are the longitudinal displacements at the base of adherend 1 and the top of adherend 2, respectively, and ta is the thickness of the adhesive layer. Using Eqs. (29) and (31) in Eq. (24), yields

$$\frac{d\tau(x)}{dx} = \frac{G_a}{t_a} \left\{ \begin{array}{c} \dfrac{du_2(x)}{dx} - \dfrac{du_1(x)}{dx} - \\ \dfrac{t_a}{(EI)_t} \cdot M_T(x) - \\ \dfrac{t_a}{(\alpha \cdot GA)_t} \cdot \dfrac{dV_T(x)}{dx} \end{array} \right\} \quad (32)$$

The strains at the base of adherent 1 and the top of adherent 2, considering of the axial force, bending moment, interfacial shear stress, shear force, are given as

$$\varepsilon_i(x) = \pm \cdot \frac{y_i}{E_i \cdot I_i} \cdot M_i(x) + \frac{N_i(x)}{E_i \cdot I_i} \pm \frac{t_i}{12 \cdot G_i} \cdot \frac{d\tau(x)}{dx} \pm \frac{y_i}{G_i \cdot A_i} \cdot \frac{dV_i(x)}{dx} \quad i = 1,2 \quad (33)$$

According to the third hypothesis, which considers that the curvature of the beam and the plate are identical, we have the following relation between the bending moments $M_1(x)$ and $M_2(x)$

$$\frac{M_1(x)}{E_1 \cdot I_1} = \frac{M_2(x)}{E_2 \cdot I_2} \Rightarrow \begin{cases} M_1(x) = R \cdot M_2(x) \\ R = \dfrac{E_1 \cdot I_1}{E_2 \cdot I_2} \end{cases} \quad (34)$$

From Eq. (1), the following relationship can be written

$$-\frac{dN_1(x)}{dx} = \frac{dN_2(x)}{dx} = b_2 \cdot \tau(x) \quad (35)$$

In which

$$-N_1(x) = N_2(x) = N(x) = b_2 \cdot \int_0^x \tau(x) \cdot dx \quad (36)$$

The total bending moment $M_T(x)$ of the infinitesimal element at a distance *x*, of the plated beam in Fig. 2 is given as follows

$$M_T(x) = M_1(x) + M_2(x) + N(x) \cdot (y_1 + y_2 + t_a) \quad (37)$$

The bending moment in each adherend, expressed as a function of the total applied moment and the interfacial shear stress, is given as

$$M_1(x) = \frac{R}{R+1}\left[M_T(x) - b_2 \int_0^x \tau(x)(y_1 + y_2 + t_a)\,dx\right] \quad (38)$$

$$M_2(x) = \frac{1}{R+1}\left[M_T(x) - b_2 \int_0^x \tau(x)(y_1 + y_2 + t_a)\,dx\right] \quad (39)$$

The first derivative of the bending moment in each adherend give

$$\frac{dM_1(x)}{dx} = V_1(x) = \frac{R}{R+1}\left[V_T(x) - b_2 \cdot \tau(x)(y_1 + y_2 + t_a)\right] \quad (40)$$

And

$$\frac{dM_2(x)}{dx} = V_2(x) = \frac{1}{R+1}[V_T(x) - b_2 \cdot \tau(x)(y_1 + y_2 + t_a)] \quad (41)$$

Substituting Eq. (33) into Eq. (32) and differentiating the resulting equation once yields

$$\frac{d\tau(x)}{dx} = \frac{G_a}{t_a} \left(\begin{array}{c} -\dfrac{y_2}{E_2.I_2}.M_2(x) + \dfrac{N_2(x)}{E_2.A_2} - \\ \dfrac{t_2}{12.G_2} \cdot \dfrac{d\tau(x)}{dx} - \dfrac{y_2}{G_2.A_2} \cdot \dfrac{dV_2(x)}{dx} - \\ \dfrac{y_1}{E_1.I_1}.M_1(x) - \dfrac{N_1(x)}{E_1.A_1} - \\ \dfrac{t_1}{12.G_1} \cdot \dfrac{d\tau(x)}{dx} - \dfrac{y_1}{G_1.A_1} \cdot \dfrac{dV_1(x)}{dx} - \\ \dfrac{t_a}{(EI)_t} \cdot M_T(x) - \\ \dfrac{t_a}{(\alpha \cdot GA)_t} \cdot \dfrac{dV_T(x)}{dx} \end{array} \right) \quad (42)$$

By rearranging Eq. (42) and introducing new parameters ξ_1 and ξ_2 we have following relationships.

$$\frac{d\tau(x)}{dx} =$$

$$K_i \left\{ \begin{array}{c} -\frac{y_2}{E_2.I_2}.M_2(x)+\frac{N_2(x)}{E_2.A_2}- \\ \frac{y_2}{G_2\cdot A_2\cdot \xi_2}\cdot\frac{dV_2(x)}{dx}-\frac{y_1}{E_1.I_1}.M_1(x)- \\ \frac{N_1(x)}{E_1.A_1}-\frac{y_1}{G_1\cdot A_1\cdot \xi_1}\cdot\frac{dV_1(x)}{dx}- \\ \frac{t_a}{(EI)_t}\cdot M_T(x)- \\ \frac{t_a}{(\alpha\cdot GA)_t}\cdot\frac{dV_T(x)}{dx} \end{array} \right\} \quad (43)$$

In which

$$\begin{cases} K_1=\frac{1}{K_i} \quad i=2,3 \\ K_2=\frac{t_a}{G_a}+\frac{t_1}{12\cdot G_1}+\frac{t_2}{12\cdot G_2} \\ K_3=\frac{t_a}{G_a} \end{cases} \quad (44)$$

Where $\xi_1=\xi_2=1$ are parameters shear deformation defined by Guenaneche (2014) and $\xi_1=\xi_2=-\frac{5}{6}$ are parameters defined by Edalati and Fereidon (2012) and Smith and Teng (2001)

K_2 coefficient defined in this paper by Guenaneche (2014) and K_3 coefficient defined by Smith and Teng (2001) and Edalati and Fereidon (2012)

Differentiating the above expression with respect to x and substituting Eqs. (34)- (41) Into Eq. (43) yields

$$\frac{d^2\tau(x)}{dx^2}-a_0\cdot\tau(x)+b_0\cdot\frac{d\sigma(x)}{dx}=f(x) \quad (45)$$

in which the constants a_0 and b_0 and function $f(x)$ are defined as follows

$$a_0=K_1\cdot\left[\frac{\frac{1}{E_1\cdot A_1}+\frac{1}{E_2\cdot A_2}+\frac{(y_1+y_2)\cdot(y_1+y_2+t_a)}{E_1\cdot I_1+E_2\cdot I_2}}{}\right]\cdot b_2 \quad (46)$$

$$b_0=\left(\frac{y_2}{\xi_2\cdot G_2\cdot A_2}-\frac{y_1}{\xi_1\cdot G_1\cdot A_1}\right)\cdot K_1\cdot b_2 \quad (47)$$

$$f(x)=-K_1\cdot\frac{(y_1+y_2+t_a)}{(E_1\cdot I_1+E_2\cdot I_2)}\cdot V_T(x)- K_1\cdot\frac{y_1}{\alpha\cdot G_1.A_1}\cdot\frac{dq}{dx}- \frac{K_1\cdot t_a}{(\alpha\cdot GA)_t}\cdot\frac{d^2V_T(x)}{dx^2} \quad (48)$$

Eq. (45) is the first differential equation cougoverning interfacial stresses for plated beam.

Differential equation for interfacial normal stresses

Due to the loading of the plated beam, the adherend 1 and the adherend 2 is subjected to distinct vertical displacements respectively $V_1(x)$ and $V_2(x)$, thus creating normal stresses in the adhesive layer.

The normal stress $\sigma(x)$ in the adhesive layer is obtained by Smith and Teng (2001) and expressed with following equation.

$$\sigma(x)=\frac{E_a}{t_a}\cdot[v_2(x)-v_1(x)] \quad (49)$$

In which E_a=elastic modulus of the adhesive layer; and t_a=thickness of the adhesive layer.

Differentiating Eq. (49) twice results in

$$\frac{d^2\sigma(x)}{dx^2}=\frac{E_a}{t_a}\cdot\left[\frac{d^2v_2(x)}{dx^2}-\frac{d^2v_1(x)}{dx^2}\right] \quad (50)$$

Considering the moment-curvature relationships for the beam and the external reinforcement, respectively, gives

$$\frac{d^2v_i(x)}{dx^2}=-\frac{1}{E_i\cdot I_i}\cdot M_i(x)\mp\frac{1}{\alpha\cdot G_i\cdot A_i}\cdot\frac{dV_i(x)}{dx} \quad i=1,2 \quad (51)$$

The equilibrium of adherents 1 and 2, leads to the following relationships:

Adherent 1

$$\frac{dM_1(x)}{dx}=V_1(x)-b_2\cdot y_1\cdot\tau(x) \quad (52)$$

$$\frac{dV_1(x)}{dx}=-b_2\cdot\sigma(x)-q(x) \quad (53)$$

Adherent 2

$$\frac{dM_2(x)}{dx}=V_2(x)-b_2\cdot y_2\cdot\tau(x) \quad (54)$$

$$\frac{dV_2(x)}{dx}=b_2\cdot\sigma(x) \quad (55)$$

Consecutively differentiating Eq. (51) and using Eqs. (52)-(55), the following expressions are obtained.

For the adherent 1:

$$\frac{d^4v_1(x)}{dx^4}=\frac{1}{E_1\cdot I_1}\cdot b_2\cdot\sigma(x)+\frac{1}{E_1\cdot I_1}\cdot q(x)+\frac{b_2\cdot y_1}{E_1\cdot I_1}\cdot\frac{d\tau(x)}{dx}-\frac{1}{\alpha\cdot G_1\cdot A_1}\cdot\frac{d^2q(x)}{dx^2}-\frac{b_2}{\alpha\cdot G_1\cdot A_1}\cdot\frac{d^2\sigma(x)}{dx^2} \quad (56)$$

For the adherent 2:

$$\frac{d^4v_2(x)}{dx^4}=-\frac{1}{E_2\cdot I_2}\cdot b_2\cdot\sigma(x)+\frac{b_2\cdot y_2}{E_2\cdot I_2}\cdot\frac{d\tau(x)}{dx}+\frac{b_2}{\alpha\cdot G_2\cdot A_2}\cdot\frac{d^2\sigma(x)}{dx^2} \quad (57)$$

By substituting Eq. (56) and Eq. (57) into the forth-order derivative of Eq. (49), we obtain the following coupled differential equation.

$$\frac{d^4\sigma(x)}{dx^4}-c_0\cdot\frac{d^2\sigma(x)}{dx^2}+d_0\cdot\sigma(x)+e_0\cdot\frac{d\tau(x)}{dx}=g(x) \quad (58)$$

In which constants c_0, d_0 and e_0 and function $g(x)$ are defined as follows

$$c_0 = \frac{E_a}{t_a} \cdot \frac{b_2}{\alpha} \cdot \left(\frac{1}{G_1 \cdot A_1} + \frac{1}{G_2 \cdot A_2}\right) \tag{59}$$

$$d_0 = \frac{E_a \cdot b_2}{t_a} \cdot \left(\frac{1}{E_1 \cdot I_1} + \frac{1}{E_2 \cdot I_2}\right) \tag{60}$$

$$e_0 = \frac{E_a \cdot b_2}{t_a} \cdot \left(\frac{y_1}{E_1 \cdot I_1} - \frac{y_2}{E_2 \cdot I_2}\right) \tag{61}$$

$$g(x) = \frac{E_a}{t_a} \cdot \frac{1}{\alpha \cdot G_1 A_1} \cdot \frac{d^2 q(x)}{dx^2} - \frac{E_a}{t_a} \cdot \frac{1}{E_1 \cdot I_1} \cdot q(x) \tag{62}$$

Eq. (58) is the second differential equation coupled governing interfacial stresses for plated beam.

3. General solution for the coupled differential equations for interfacial stresses

The Eqs. (48) and (58) form a system of coupled differential equations. To decouple Eqs. (48) and (58), we use the method defined in the paper of Edalati and Fereidon (2012) by multiplying the Eq. (48) by $-e_0 \cdot \frac{d}{dx}$ and Eq. (58) by $\frac{d^2}{dx^2} - a_0$. The interfacial shear stress $\tau(x)$ is this eliminated in the inhomogeneous coupled differential Eqs. (48) and (58). The solution obtained is given by the following expression.

$$\frac{d^6\sigma(x)}{dx^6} - (a_0 + c_0) \cdot \frac{d^4\sigma(x)}{dx^4} + (a_0 \cdot c_0 + d_0 - b_0 \cdot e_0) \cdot \frac{d^2\sigma(x)}{dx^2} - a_0 \cdot d_0 \cdot \frac{d\sigma(x)}{dx} = \frac{d^2 g(x)}{dx^2} - a_0 \cdot g(x) - e_0 \cdot \frac{df(x)}{dx} = F(x) \tag{63}$$

By multiplying the Eq. (48) by $\frac{d^4}{dx^4} - c_0 \cdot \frac{d^2}{dx^2} + d_0$ and Eq. (58) by $-b_0 \cdot \frac{d}{dx}$. The interfacial shear stress $\sigma(x)$ is this eliminated in the inhomogeneous coupled differential Eqs. (48) and (58). Then

$$\frac{d^6\tau(x)}{dx^6} - (a_0 + c_0) \cdot \frac{d^4\tau(x)}{dx^4} + (a_0 \cdot c_0 + d_0 - b_0 \cdot e_0) \cdot \frac{d^2\tau(x)}{dx^2} - a_0 \cdot d_0 \cdot \frac{d\tau(x)}{dx} = \frac{d^4 f(x)}{dx^4} - c_0 \cdot \frac{d^2 f(x)}{dx^2} + d_0 \cdot \frac{df(x)}{dx} - b_0 \cdot \frac{dg(x)}{dx} = G(x) \tag{64}$$

The equation characteristic of the differential Eq. (63) is the same as that of Eq. (64). It is given by the following relationship

$$r^6 - (a_0 + c_0) \cdot r^4 + (a_0 \cdot c_0 + d_0 - b_0 \cdot e_0) \cdot r^2 - a_0 \cdot d_0 = 0 \tag{65}$$

Using a change of variables, $= r^2$, obtains

$$m^3 - (a_0 + c_0) \cdot m^2 + (a_0 \cdot c_0 + d_0 - b_0 \cdot e_0) \cdot m - a_0 \cdot d_0 = 0 \tag{66}$$

To solve this equation we use the method of Tartaglia-Cardan cited in Wikipedia (2018). By eliminating the second term of this equation, it is given by the following expression

$$m^3 + \frac{n_2}{3} \cdot m - \frac{n_1}{27} = 0 \tag{67}$$

Where n_1 and n_2 are given by followings relationships

$$n_1 = 2 \cdot a_0^3 - 3 \cdot a_0^2 \cdot c_0 - 3 \cdot a_0 \cdot c_0^2 + 2 \cdot c_0^3 + 18 \cdot a_0 \cdot d_0 - 9 \cdot c_0 \cdot d_0 + 9 \cdot a_0 \cdot b_0 \cdot e_0 + 9 \cdot b_0 \cdot c_0 \cdot e_0 \tag{68}$$

$$n_2 = -a_0^2 + a_0 \cdot c_0 - c_0^2 + 3 \cdot d_0 - 3 \cdot b_0 \cdot e_0 \tag{69}$$

The solutions of this Eq. (67) depend on the following Δ parameter.

$$\Delta = \frac{n_1^2 + 4 \cdot n_2^3}{27^2} \tag{70}$$

If Δ is positive yield three solutions

$$m_1 = \frac{1}{3} \cdot \left[a_0 + c_0 - \frac{\sqrt[3]{2} \cdot n_2}{n_3} + \frac{n_3}{\sqrt[3]{2}}\right] \tag{71}$$

$$m_2 = \frac{1}{3} \cdot \begin{bmatrix} a_0 + c_0 + \frac{(1 + i\sqrt{3}) \cdot n_2}{\sqrt[3]{4} \cdot n_3} - \\ \frac{(1 - i\sqrt{3}) \cdot n_3}{2 \cdot \sqrt[3]{2}} \end{bmatrix} \tag{72}$$

$$m_3 = \frac{1}{3} \cdot \begin{bmatrix} a_0 + c_0 + \frac{(1 - i\sqrt{3}) \cdot n_2}{\sqrt[3]{4} \cdot n_3} - \\ \frac{(1 + i\sqrt{3}) \cdot n_3}{2 \cdot \sqrt[3]{2}} \end{bmatrix} \tag{73}$$

Where m_1 is positive real number and m_2, m_3 are conjugate complex numbers.

The parameter n_3 is defined by following relationship

$$n_3 = \sqrt[3]{n_1 + \sqrt{n_1^2 + 4 \cdot n_2^3}} \tag{74}$$

The solutions of the differential Eqs. (63) and (64) are given by the following expressions.

$$\sigma(x) = C_1 \cdot e^{-\psi_1 \cdot x} + e^{-\psi_2 \cdot x} \cdot \begin{bmatrix} C_2 \cdot \cos(\psi_3 \cdot x) + \\ C_3 sin(\psi_3 \cdot x) \end{bmatrix} + C_4 \cdot e^{\psi_1 \cdot x} + e^{\psi_2 \cdot x} \cdot \begin{bmatrix} C_5 \cdot \cos(\psi_3 \cdot x) + \\ C_6 sin(\psi_3 \cdot x) \end{bmatrix} - \frac{F(x)}{a_0 \cdot d_0} \tag{75}$$

$$\tau(x) = K_1 \cdot e^{-\psi_1 \cdot x} + e^{-\psi_2 \cdot x} \cdot \begin{bmatrix} K_2 \cdot \cos(\psi_3 \cdot x) + \\ K_3 sin(\psi_3 \cdot x) \end{bmatrix} + K_4 \cdot e^{\psi_1 \cdot x} + e^{\psi_2 \cdot x} \cdot \begin{bmatrix} K_5 \cdot \cos(\psi_3 \cdot x) + \\ K_6 sin(\psi_3 \cdot x) \end{bmatrix} - \frac{G(x)}{a_0 \cdot d_0} \tag{76}$$

Where C_1 to C_6 and K_1 to K_6 are the constants of

integration which can be determined from appropriate boundary conditions.

The coefficients ψ_1, ψ_2 *and* ψ_3 are obtained by the following expressions

$$\psi_1 = \sqrt{m_1} \tag{77}$$

$$\psi_2 = \sqrt{0.5 \cdot (\sqrt{\chi_1^2 + \chi_2^2} + \chi_1)} \tag{78}$$

$$\psi_3 = \frac{\chi_2}{2 \cdot \psi_2} \tag{79}$$

Where χ_1, χ_2, are respectively real and imaginary of complex number m_2 and m_3

$$\chi_1 = \frac{1}{3} \cdot [a_0 + c_0 + \frac{n_2}{\sqrt[3]{4} \cdot n_3} - \frac{n_3}{2 \cdot \sqrt[3]{2}}] \tag{80}$$

$$\chi_2 = \frac{1}{3} \cdot [\frac{\sqrt{3} \cdot n_2}{\sqrt[3]{4} \cdot n_3} + \frac{n_3 \cdot \sqrt{3}}{2 \cdot \sqrt[3]{2}}] \tag{81}$$

The positive exponential terms in Eqs. (75) and (76) are considered neglected by Narayamurty (2016) for almost all practical plated beams so that $C_4 = C_5 = C_6 = K_4 = K_5 = K_6 = 0$. The expressions of $\tau(x)$ and $\sigma(x)$ are simplified.

$$\sigma(x) = C_1 \cdot e^{-\psi_1 \cdot x} + e^{-\psi_2 \cdot x} \cdot [\begin{matrix} C_2 \cdot \cos(\psi_3 \cdot x) + \\ C_3 sin(\psi_3 \cdot x) \end{matrix}] - \frac{F(x)}{a_0 \cdot d_0} \tag{82}$$

$$\tau(x) = K_1 \cdot e^{-\psi_1 \cdot x} + e^{-\psi_2 \cdot x} \cdot [\begin{matrix} K_2 \cdot \cos(\psi_3 \cdot x) + \\ K_3 sin(\psi_3 \cdot x) \end{matrix}] - \frac{G(x)}{a_0 \cdot d_0} \tag{83}$$

By simultaneous substitution of Eqs. (82) and (83) into one of the coupled differential Eq. (45), the constants K_1 through K_3 can be evaluated as functions of C_1 through C_3

$$\begin{aligned} K_1 &= \frac{b_0 \cdot \psi_1 \cdot C_1}{\psi_1^2 - a_0} \\ K_2 &= \delta_5 \cdot C_2 + \delta_6 \cdot C_3 \\ K_3 &= -\delta_6 \cdot C_2 + \delta_5 \cdot C_3 \end{aligned} \tag{84}$$

Where $\lambda_1, \delta_1, \delta_2, \delta_3, \delta_4, \delta_5$ *and* δ_6 are given by following relationships

$$\lambda_1 = \frac{b_0 \cdot \psi_1}{\psi_1^2 - a_0} \tag{85}$$

$$\begin{aligned} \delta_1 &= \psi_2^2 - \psi_3^2 - a_0 \\ \delta_2 &= 2 \cdot \psi_2 \cdot \psi_3 \\ \delta_3 &= b_0 \cdot \psi_2 \\ \delta_4 &= b_0 \cdot \psi_3 \end{aligned} \tag{86}$$

$$\delta_5 = \frac{\delta_1 \cdot \delta_3 + \delta_2 \cdot \delta_4}{\delta_1^2 + \delta_2^2} \quad , \quad \delta_6 = \frac{\delta_2 \cdot \delta_3 - \delta_1 \cdot \delta_4}{\delta_1^2 + \delta_2^2} \tag{87}$$

If Δ is negative, then m_4, m_5 and m_6 are positive real numbers, the solutions of differential Eqs. (63) and (64) are expressed by following relationships

$$\sigma(x) = C_7 \cdot e^{-\psi_4 \cdot x} + C_8 \cdot e^{\psi_4 \cdot x} + C_9 \cdot e^{-\psi_5 \cdot x} + C_{10} \cdot e^{\psi_5 \cdot x} + C_{11} \cdot e^{-\psi_6 \cdot x} + C_{12} \cdot e^{\psi_6 \cdot x} - \frac{F(x)}{a_0 \cdot d_0} \tag{88}$$

$$\tau(x) = K_7 \cdot e^{-\psi_4 \cdot x} + K_8 \cdot e^{\psi_4 \cdot x} + K_9 \cdot e^{-\psi_5 \cdot x} + K_{10} \cdot e^{\psi_5 \cdot x} + K_{11} \cdot e^{-\psi_6 \cdot x} + K_{12} \cdot e^{\psi_6 \cdot x} - \frac{G(x)}{a_0 \cdot d_0} \tag{89}$$

Where the parameters $\psi_i, i = 4{,}5$ and 6 are determined by the solutions of the equation characteristic of the differential Eq. (63).

$$\psi_i = \sqrt{m_i} \quad i = 4{,}5 \quad and \quad 6 \tag{90}$$

The constants *K*7 through *K*12 can be evaluated as functions of *C*7 through *C*12

$$K_i = \frac{b_0 \cdot \psi_i \cdot C_i}{\psi_i^2 - a_0} \quad i = 7{,}12 \tag{91}$$

The positive exponential terms in Eqs. (75) and (76) are considered neglected by Narayamurty (2016) for almost all practical plated beams so that $C_8 = C_{10} = C_{12} = K_8 = K_{10} = K_{12} = 0$. The expressions of $\tau(x)$ and $\sigma(x)$ are simplified.

$$\sigma(x) = C_7 \cdot e^{-\psi_4 \cdot x} + C_9 \cdot e^{-\psi_5 \cdot x} + C_{11} \cdot e^{-\psi_6 \cdot x} - \frac{F(x)}{a_0 \cdot d_0} \tag{92}$$

$$\tau(x) = K_7 \cdot e^{-\psi_4 \cdot x} + K_9 \cdot e^{-\psi_5 \cdot x} + K_{11} \cdot e^{-\psi_6 \cdot x} - \frac{G(x)}{a_0 \cdot d_0} \tag{93}$$

3.1 General boundary conditions

The general boundary conditions are expressed by the following relations

$$N_1(0) = N_2(0) = M_2(0) = 0 \tag{94}$$

$$M_1(0) = M_T(0) \tag{95}$$

$$V_2(0) = 0 \quad , \quad V_1(0) = V_T(0) \tag{96}$$

Substitution of Eqs. (94) and (95) into Eq. (43) gives Eq. (97). The same manner by substitution of the Eqs. (51) and (95) into the second derivative of Eq. (49) with respect to *x* gives Eq. (98). Finally substitution of the third derivative of Eq. (51) with respect to *x* into right side of the third derivative of Eq. (49) with respect to *x* and using Eq. (96) arrives at Eq. (99).

$$b_0 \cdot \sigma(x)|_{x=0} + \frac{d\tau(x)}{dx}|_{x=0} = f_1(x)|_{x=0} + g_1(x)|_{x=0} \tag{97}$$

$$-c_0 \cdot \sigma(x)|_{x=0} + \frac{d^2\sigma(x)}{dx^2}|_{x=0} = h_1(x)|_{x=0} + m_1(x)|_{x=0} \tag{98}$$

$$e_0 \cdot \tau(x)|_{x=0} - \quad c_0 \cdot \frac{d\sigma(x)}{dx}|_{x=0} + \frac{d^3\sigma(x)}{dx^3}|_{x=0} = \quad n_1(x)|_{x=0} \tag{99}$$

The functions $f_1(x)$, $g_1(x)$, $h_1(x)$, $m_1(x)$ and $n_1(x)$ depend on the applied load.

$$f_1(x)|_{x=0} = -K_1 \cdot \left[\frac{\frac{y_1}{E_1 \cdot I_1} + \frac{t_a}{E_1 \cdot I_1 + E_2 \cdot I_2}}{}\right] \cdot M_T(x)|_{x=0} \tag{100a}$$

$$g_1(x)|_{x=0} = K_1 \cdot \left[\frac{\frac{y_1}{G_1 \cdot A_1} + \frac{t_a}{\alpha \cdot (G_1 \cdot A_1 + G_2 \cdot A_2)}}{}\right] \cdot q(x)|_{x=0} \tag{100b}$$

$$h_1(x)|_{x=0} = \frac{E_a}{t_a} \cdot \frac{1}{E_1 \cdot I_1} \cdot M_T(x)|_{x=0} \tag{100c}$$

$$m_1(x)|_{x=0} = \frac{E_a}{t_a} \cdot \frac{1}{\alpha \cdot G_1 \cdot A_1} \cdot q(x)|_{x=0} \tag{100d}$$

$$n_1(x)|_{x=0} = \frac{E_a}{t_a} \cdot \frac{1}{E_1 \cdot I_1} \cdot V_T(x)|_{x=0} \tag{100e}$$

$$r_1(x)|_{x=0} = \frac{E_a}{t_a} \cdot (\frac{1}{\alpha \cdot G_1 \cdot A_1}) \cdot \frac{dq(x)}{dx}|_{x=0} \tag{100f}$$

3.1.1 Calculating constants C1 through C3 in the Δ positive case

By substituting $\tau(x)|_{x=0}$, $\sigma(x)|_{x=0}$, $\frac{d\tau(x)}{dx}|_{x=0}$. $\frac{d\sigma(x)}{dx}|_{x=0}$, $\frac{d^2\sigma(x)}{dx^2}|_{x=0}$ and $\frac{d^3\sigma(x)}{dx^3}|_{x=0}$ in Eqs. (95), (96) and (97) we obtain a system of three equations with three unknowns C_1, C_2 and C_3

$$\begin{cases} (b_0 - \frac{b_0 \cdot \psi_1^2}{\psi_1^2 - a_0}) \cdot C_1 + (b_0 - \psi_2 \cdot \delta_5 - \psi_3 \cdot \delta_6) \cdot C_2 + (\psi_3 \cdot \delta_5 - \psi_2 \cdot \delta_6) \cdot C_3 = z_1 \\ (\psi_1^2 - c_0) \cdot C_1 + (\psi_2^2 - \psi_3^2 - c_0) \cdot C_2 - 2 \cdot \psi_2 \cdot \psi_3 \cdot C_3 = z_2 \\ (\frac{e_0 \cdot \psi_1 \cdot b_0}{\psi_1^2 - a_0} + c_0 \cdot \psi_1 - \psi_1^3) \cdot C_1 + (e_0 \cdot \delta_5 + c_0 \cdot \psi_2 - \psi_2^3 + 3 \cdot \psi_2 \cdot \psi_3^2) \cdot C_2 \\ +(e_0 \cdot \delta_6 - c_0 \cdot \psi_3 - \psi_3^3 + 3 \cdot \psi_2^2 \cdot \psi_3) \cdot C_3 = z_3 \end{cases} \tag{101}$$

Where Z_1 Z_2, and Z_3 depend on the applied load

$$z_1 = \frac{b_0}{a_0 \cdot d_0} \cdot \quad F(x)|_{x=0} - \frac{1}{a_0 \cdot d_0} \cdot \frac{dG(x)}{dx}|_{x=0} + \quad f_1(x)|_{x=0} + \quad g_1(x)|_{x=0} \tag{102}$$

$$z_2 = -\frac{c_0 \cdot F(x)}{a_0 \cdot d_0}|_{x=0} + \frac{1}{a_0 \cdot d_0} \cdot \frac{d^2F(x)}{dx^2}|_{x=0} + h_1(x)|_{x=0} + m_1(x)|_{x=0} \tag{103}$$

$$z_3 = \frac{e_0 \cdot \quad G(x)|_{x=0}}{a_0 \cdot d_0} - \frac{c_0}{a_0 \cdot d_0} \cdot \quad \frac{dF(x)}{dx}|_{x=0} + \frac{1}{a_0 \cdot d_0} \cdot \frac{d^3F(x)}{dx^3}|_{x=0} + n_1(x)|_{x=0} + r_1(x)|_{x=0} \tag{104}$$

The analytical relationships for C_1, C_2, and C_3 can be calculated using free mathematical code (GNU Octave) or commercial mathematical code (Matlab or Maple).

3.1.2 Calculating constants C1 through C3 in the Δ negative case

By substituting $\tau(x)|_{x=0}$, $\sigma(x)|_{x=0}$, $\frac{d\tau(x)}{dx}|_{x=0}$. $\frac{d\sigma(x)}{dx}|_{x=0}$, $\frac{d^2\sigma(x)}{dx^2}|_{x=0}$ and $\frac{d^3\sigma(x)}{dx^3}|_{x=0}$ in Eqs. (95), (96) and (97) we obtain a system of three equations with three unknowns C_7 C_9 , and C_{11}

$$\begin{cases} (\frac{1}{\psi_4^2 - a_0}) \cdot C_7 + (\frac{1}{\psi_5^2 - a_0}) \cdot C_9 + (\frac{1}{\psi_6^2 - a_0}) \cdot C_{11} = z_1 \\ (\psi_4^2 - a_0) \cdot C_7 + (\psi_5^2 - a_0) \cdot C_9 + (\psi_6^2 - a_0) \cdot C_{11} = z_2 \\ (\frac{b_0 \cdot e_0 \cdot \psi_4}{\psi_4^2 - a_0} + c_0 \cdot \psi_4 - \psi_4^3) \cdot C_7 + (\frac{b_0 \cdot e_0 \cdot \psi_5}{\psi_5^2 - a_0} + c_0 \cdot \psi_5 - \psi_5^3) \cdot C_9 + \\ (\frac{b_0 \cdot e_0 \cdot \psi_4}{\psi_6^2 - a_0} + c_0 \cdot \psi_6 - \psi_6^3) \cdot C_{11} = z_3 \end{cases} \tag{105}$$

Where Z_1, Z_2 and Z_3 depend on the applied load. The expressions of Z_1, Z_2 and Z_3 are identical to those given by Eqs. (102), (103) and (104).

The analytical relationships for C_7, C_9, and C_{11} can be calculated using free mathematical code (GNU Octave) or commercial mathematical code (Matlab or Maple).

3.1.3 Calculating the parameters z1, z2 and z3 for UDL case

The relations of the total shear force and the total bending moment, in the case of UDL $[q(x) = q]$ are as follows

$$V_T(x) = \frac{q}{2} \cdot (L_p - 2 \cdot x) \tag{106}$$

$$M_T(x) = \frac{q}{2} \cdot [x \cdot (L_p - 2 \cdot x) + L_{fs} \cdot (L_p + L_{fs})] \tag{107}$$

For $0 \leq x \leq L_p$

Substituting Eq. (106) in Eq. (49) we obtain the following relationship

$$f(x) = -\frac{K_1 \cdot q}{2} \cdot \frac{(y_1 + y_2 + t_a)}{(E_1 \cdot I_1 + E_2 \cdot I_2)} \cdot (L_p - 2 \cdot x) \quad (108)$$

The loading of the plated beam being uniform and constant $[q(x) = q]$, Eq. (63) takes the following form

$$g(x) = -\frac{E_a}{t_a} \cdot \frac{1}{E_1 \cdot I_1} \cdot q \quad (109)$$

Substituting Eqs. (108) and (109) in Eqs. (63a) and (64a) gives the following relationships

$$F(x) = \frac{E_a}{t_a} \cdot \frac{q \cdot a_0}{E_1 \cdot I_1} - K_1 \cdot q \cdot e_0 \cdot \frac{(y_1 + y_2 + t_a)}{(E_1 \cdot I_1 + E_2 \cdot I_2)} \quad (110)$$

$$G(x) = K_1 \cdot q \cdot d_0 \cdot \frac{(y_1 + y_2 + t_a)}{(E_1 \cdot I_1 + E_2 \cdot I_2)} \quad (111)$$

By substituting $q(x)|_{x=0}$, $\frac{d^2q(x)}{dx^2}|_{x=0}$, $V(x)|_{x=0}$, $\frac{dV(x)}{dx}|_{x=0}$, $M(x)|_{x=0}$, $F(x)|_{x=0}$, $G(x)|_{x=0}$, $\frac{dF(x)}{dx}|_{x=0}$, $\frac{dG(x)}{dx}|_{x=0}$, $\frac{d^2F(x)}{dx^2}|_{x=0}$, $\frac{d^3F(x)}{dx^3}|_{x=0}$, $f_1(x)|_{x=0}, g_1(x)|_{x=0}, h_1(x)|_{x=0}, m_1(x)|_{x=0}, n_1(x)|_{x=0}$, and $r_1(x)|_{x=0}$ in Eqs. (102), (103) and (104) we obtain the following equations of parameters z_1, z_2 and z_3

$$z_1 = \frac{E_a}{t_a \cdot d_0} \cdot \frac{q \cdot b_0}{E_1 \cdot I_1} - \frac{K_1 \cdot q \cdot b_0 \cdot e_0}{a_0 \cdot d_0} \cdot \frac{(y_1 + y_2 + t_a)}{(E_1 \cdot I_1 + E_2 \cdot I_2)} - \frac{K_1 \cdot q \cdot L_{fs} \cdot (L_p + L_{fs})}{2} \cdot \left[\frac{y_1}{E_1 \cdot I_1} + \frac{t_a}{E_1 \cdot I_1 + E_2 \cdot I_2}\right] + K_1 \cdot q \cdot \left[\frac{y_1}{G_1 \cdot A_1} + \frac{t_a}{\alpha \cdot (G_1 \cdot A_1 + G_2 \cdot A_2)}\right] \quad (112)$$

$$z_2 = -\frac{c_0}{a_0 \cdot d_0}\left[\frac{E_a}{t_a} \cdot \frac{q \cdot a_0}{E_1 \cdot I_1} - K_1 \cdot q \cdot e_0 \cdot \frac{(y_1 + y_2 + t_a)}{(E_1 \cdot I_1 + E_2 \cdot I_2)}\right] - \frac{E_a}{t_a} \cdot \frac{1}{E_1 \cdot I_1} \cdot \frac{q \cdot L_{fs} \cdot (L_p + L_{fs})}{2} + \frac{E_a}{t_a} \cdot \frac{q}{\alpha \cdot G_1 \cdot A_1} \quad (113)$$

$$z_3 = \frac{e_0}{a_0 \cdot d_0} \cdot K_1 \cdot q \cdot d_0 \cdot \frac{(y_1 + y_2 + t_a)}{(E_1 \cdot I_1 + E_2 \cdot I_2)} + \frac{E_a}{t_a} \cdot \frac{1}{E_1 \cdot I_1} \cdot \frac{q \cdot L_p}{2} \quad (114)$$

3.1.4 Calculating the parameters z_1, z_2 and z_3 for one concentrated load case

For a point load, two domains are defined (see Fig. 4). The computation of the interface stresses in domain 1 (Fig. 4 Section 1) is similar to that of the plated beam subjected to uniform loading. In order to calculate the interfacial stresses in the domain 2 represented by section 2, Fig. 4 is turned over and the direction of the *x*-axis is changed. This method makes it possible to avoid the use of the continuity conditions at the point of application of the concentrated load and the boundary conditions at the right end of the plate. With this technique, the integration constants are easily obtained.

The relations of the total shear force and the total bending moment, in the case of single point load are in

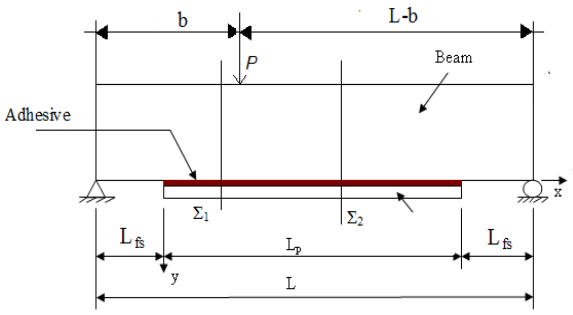

Fig. 4 Simply supported beam bonded with a soffit plate under a point load

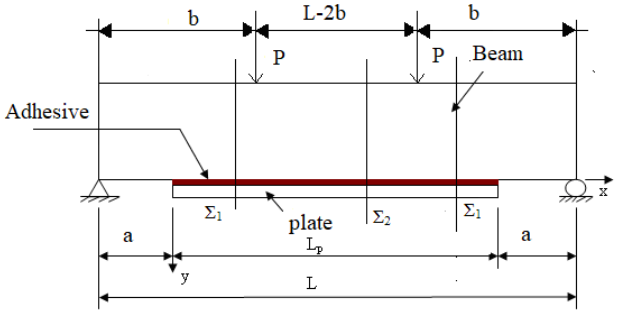

Fig. 5 Simply supported beam bonded with a soffit plate under a point load a two point loads

domain 1 as follows:

For $0 \le x \le b - L_{fs}$ $V_T(x) = \frac{P}{L}.(L - b)$ and

$$M_T(x) = \frac{P \cdot (L - b)}{L} \cdot (L_{fs} + x) \quad (115)$$

The parameters z_1, z_2 and z_3 are given by following equations.

$$z_1 = -\frac{K_1 \cdot P \cdot L_{fs} \cdot (L - b)}{L} \cdot \left[\frac{\frac{y_1}{E_1 \cdot I_1} + \frac{t_a}{E_1 \cdot I_1 + E_2 \cdot I_2}}{E_1 \cdot I_1 + E_2 \cdot I_2}\right] \quad (116)$$

$$z_2 = \frac{E_a}{t_a} \cdot \frac{1}{E_1 \cdot I_1} \cdot \frac{P \cdot L_{fs} \cdot (L - b)}{L} \quad (117)$$

$$z_3 = \frac{E_a}{t_a} \cdot \frac{1}{E_1 \cdot I_1} \cdot \frac{P \cdot (L - b)}{L} \quad (118)$$

3.1.5 Calculating the parameters z_1, z_2 and z_3 for two concentrated load

To determine the interfacial stresses in the case of a plated beam subjected to two concentrated loads (Fig. 5) the superposition principle is used. The calculation of the normal and shear stresses in the case of Figs. 6 and 7 is similar to that of the point load.

4. Comparison of interfacial stress and discussion

In this section, the results of the present method for interfacial stress are checked for accuracy. For that, two

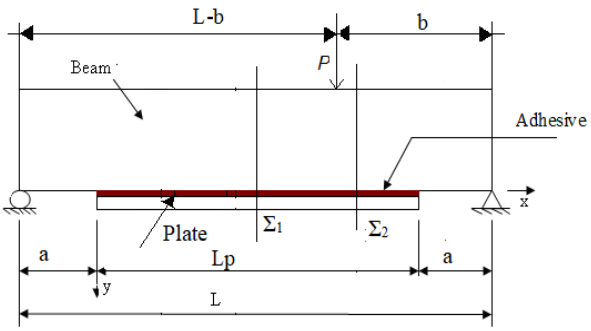

Fig. 6 Simply supported beam bonded with a soffit plate under a point load

Table1 Material and geometric properties

	Stephen *et al.* (2008)	Present with shear lag (stage 4)	Present without shear lag (stage 2)
Beam 10 series C	2.12	2.297	4.445
Beam 12 series D	2.14	2.75	3.976
Beam 19 series F	1.381	1.326	2.303
Beam 20 series F	1.05	1.697	2.922

comparisons are made. The first results are compared with theoretical solutions and the second with experimental results. In this comparison we distinguish four stages:

Stage 1: the interfacial stresses are calculated with theory of Timoshenko beam without the effect of the reduced second moment of area.

Stage 2: the interfacial stresses are calculated with theory of Timoshenko beam with the effect of the reduced second moment of area.

Stage 3: the interfacial stresses are calculated with shear deformation obtained with theory of elasticity without the effect of the reduced second moment of area.

Stage 4: the interfacial stresses are calculated with shear deformation obtained with theory of elasticity with the effect of the reduced second moment of area.

4.1 Comparison with theoretical solutions

A simply supported beam subjected to a single point load or a uniformly distributed load is considered. The RC beam is assumed to be bonded with a CFRP soffit plate. A summary of the material and geometric properties is shown in Table 1. The span of RC beam is L=3000 mm, the distance from the support to the end of the plate is a=300 mm, the mid-point load is 150 KN and UDL is 50 KN/m.

To validate the present analysis, direct comparisons are made between our results and the existing closed-form solutions. For that, the present interfacial stresses are compared with the solution of Smith and Teng (2001) where the effect of adherend shear deformations is not taken into consideration, the analytical method of Edalati and Fereidoon (2012) where the shear deformations where included in beam, adhesive layer and soffit plate, the solution of Yang and Wu (2007) which takes into account the transverse shear deformation in both the concrete beam and bonded plate, the solution of Guenaneche *et al*. (2014)

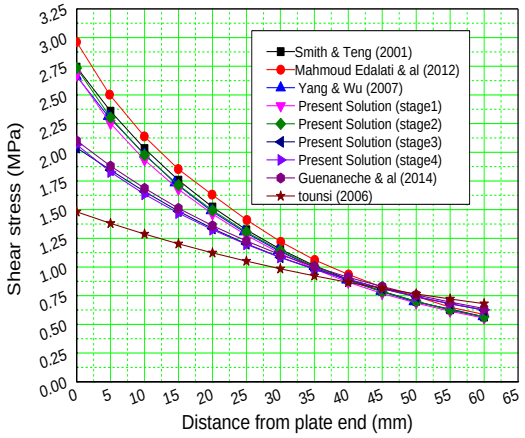

Fig. 7 Comparison of interfacial shear stresses for an RC beam with a bonded CFRP soffit plate subjected to a uniformly distributed load (UDL)

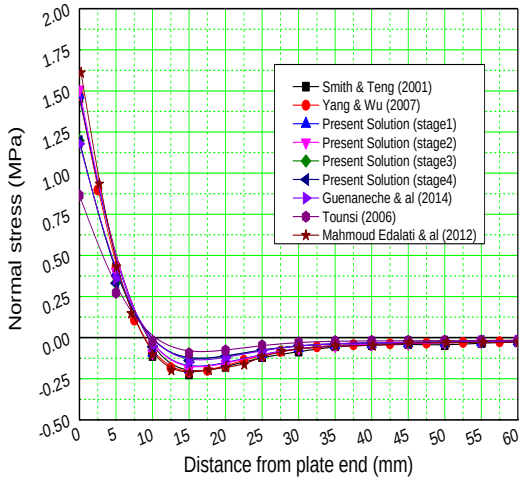

Fig. 8 Comparison of interfacial normal stresses for an RC beam with a bonded CFRP soffit plate subjected to a uniformly distributed load (UDL)

where the variation of the shear stresses induced by adherends shear deformations effect is obtained directly from the equilibrium equations of stresses and finally the theoretical solution of Tounsi (2006) where the adherend shear deformations have been included with a linear variation across the thickness.

The interfacial shear and normal stress distributions in the concrete beam bonded with CFRP soffit plate subjected to a uniformly distributed load (UDL) of the present method are compared in Fig. 7 and Fig. 8 with other previously mentioned solutions.

From these figures, it can be seen that the highest values of the interfacial stresses are obtained by the solution of Edalati and Fereidoon (2012) and present solution in stage 1 and 2 and the lower are given by the solution of Tounsi (2006).

The interfacial stresses calculated from the other solutions including the present are between the two aforementioned methods. In addition, the results of this method in stage 3 and 4 coincide perfectly with those of Guenaneche *et al*. (2014). The difference which exists

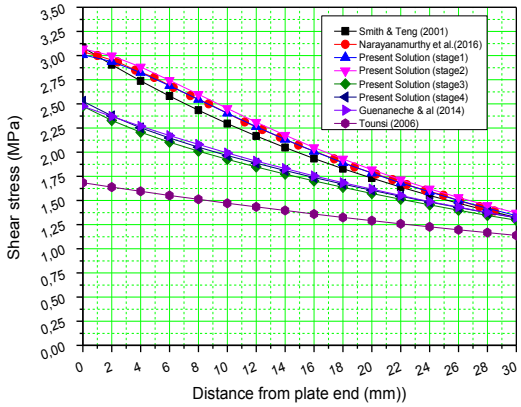

Fig. 9 Comparison of interfacial shear stresses for an RC beam with a bonded CFRP soffit plate subjected to a single point load (SPL)

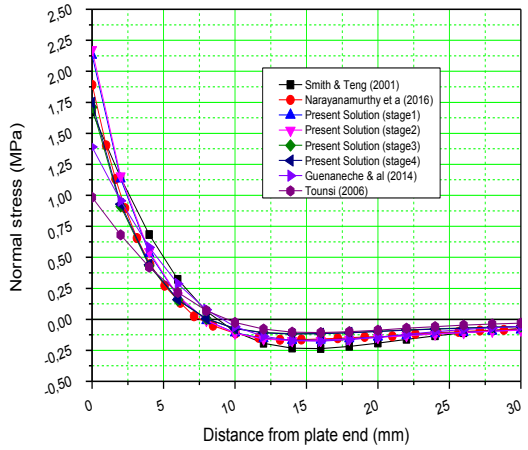

Fig. 10 Comparison of interfacial normal stresses for an RC beam with a bonded CFRP soffit plate subjected to a single point load (SPL).

between the results of the different solutions can be explained by the taking or not of the shear deformations in the adherents namely beam, soffit plate and adhesive layer and the way in which the latter has been formulated.

A second comparison of the interface stresses of the present method with those of the literature is presented in Figs. 9 and 10. This time the beam is subjected to a single point load (SPL) of a value 150 Kn. The same observation as in the case of a distributed load is observed.

Therefore, it is clear that the inclusion of shear deformations reduces the concentration of interface stresses and leads to a more uniform distribution.

In a general, we can say that there is a concordance between the different results.

4.2 Comparison with experimental results

In this section another comparison of the results of the present method is made. Four beams bonded with a FRP plate tested by Stephen *et al*. (2008), beam 10 of the series C, beam 12 of the series D and the beams 19 and 20 of the series F, were analyzed here using the present improved solution. The schema of beams 10, 12, 19 and 20 is presented in Fig. 5.

A summary of the geometric and material properties of the beams and FRP plate are listed below:

The Young modulus of FRP plate and the adhesive layer are respectively is 259000 MPa and 2960 MPa. The thickness of the adhesive is 0,5 mm.

Series F Beams 19 and 20: $f\,c$=55 MPa, FRP tp=0.330 mm, FRP length Lp=2,235 mm

Series C Beam 10: $f\,c$=21 MPa, FRP tp=0.660 mm, FRP length Lp=2,235 mm

Series D Beam 12: $f\,c$=21 MPa, FRP tp=0.660 mm, FRP length Lp=2,235 mm

The comparison of the peak interfacial shear stresses is given in Table 2. From this table, it is clear the results of the present method with the taking into account of shear lag effect (shear deformations in the adherents) are in excellent agreement with the experimental results. However, there is a significant gap with those without taking into account the shear lag effect. This confirms what was involved earlier than the inclusion of shear deformations reduces the concentration of interface stresses.

5. Theoretical parametric study

In this section, numerical results are presented to study and analyze the effect of various parameters on the distributions of the interfacial stresses in an RC beam bonded with an FRP plate.

5.1 Effect of elasticity modulus of the strengthening plate

Figures give interfacial normal and shear stresses for the RC beam bonded with FRP plate. Different Young's modulus values are used which demonstrate the effect of plate material properties on interfacial stresses.

As can be seen from this figure; when the plate material becomes stiffer, the interfacial stresses increase. This is because, under the same load, the tensile force developed in the plate is bigger, which leads to increase interfacial stresses.

5.2 Effect of the plate thickness

In Fig. 11we represent the effect of the plate thickness on the interfacial stresses. This parameter is very important in design practice. From this figure, it can be seen that peak stresses are very influenced by the variation of the thickness of the FRP plate. It is shown that the interfacial stresses increase as the thickness of FRP plate increases.

5.3 Effect the adhesive layer thickness

The effects of the thickness, of the adhesive layer on the interfacial stresses, is represented in Fig. 12 .It can be seen that increasing the thickness of the adhesive layer leads to significant reduction in the peak interfacial stresses. Thus it is recommended to use a variable thickness of the adhesive layer. In the vicinity of the edge, where the stresses are high, it is recommended using thick adhesive layer.

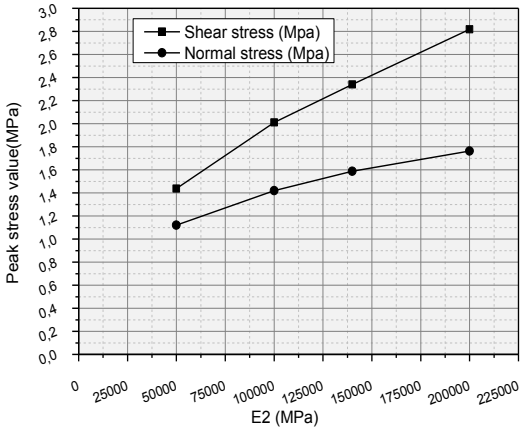

Fig. 11 Effect of the Young modulus of the FRP plate on interfacial stresses in strengthened beam

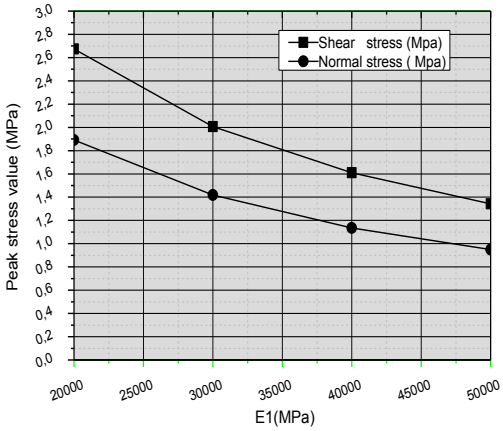

Fig. 14 Effect of the elasticity modulus of the RC beam on interfacial stresses

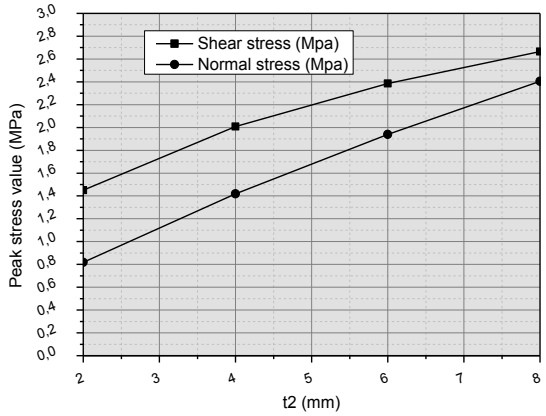

Fig. 12 Effect of plate thickness on interfacial stresses

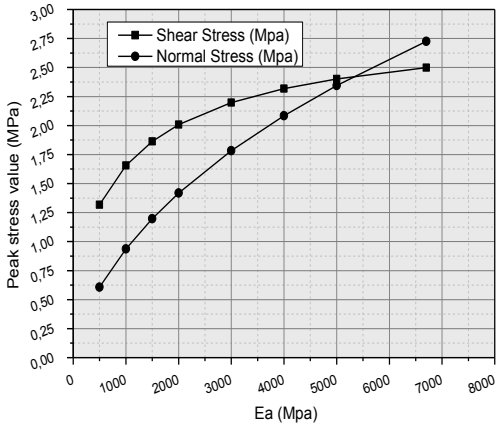

Fig. 15 Effect of the elasticity modulus of the adhesive layer on interfacial stresses

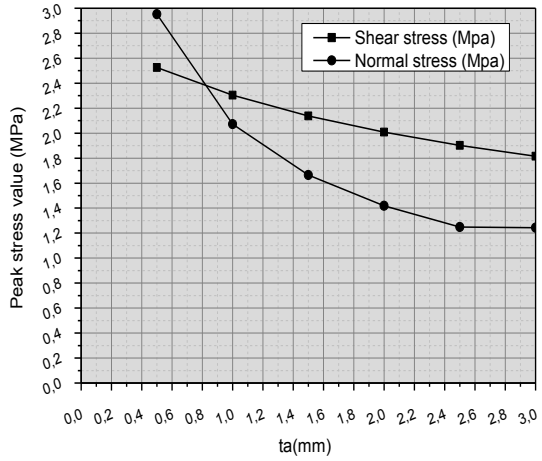

Fig. 13 Effect of the adhesive layer thickness on interfacial stresses

5.4 Effect of the elasticity modulus of the RC beam

The effects of Young's modulus of the RC beam on the interfacial edge stresses are shown in Fig. 14

As seen, the stresses decrease when the Young modulus of the RC beam increases. Hence, a RC beam with a higher modulus and strength is suggested for reducing the level and concentration of interfacial stresses.

5.5 Effect of the elasticity modulus of the adhesive layer

The adhesive layer is a relative soft isotropic material with a low stiffness. In Fig. 15 we depict the variation of the peak interfacial stresses versus the elasticity modulus of the adhesive layer.

The figure revels that the peak stresses at the end of the plate increase as Young's modulus of the adhesive increases.

6. Conclusions

The deboning failure in plated beams plates is due to the high concentrations of the stresses at the edges. It is therefore very important to quantify these stresses in order to save the reinforced structures. In this paper interfacial stresses in FRP-RC beam were studied by an accurate analytical method taking account the effect of shear deformations by using the equilibrium equations of the elasticity. The solution has been developed including stress-strain and strain-displacement relationships for the adhesive and adherends. The resolution of the coupled differential equations gives new explicit closed-form solution including

shear deformations effects. A comparison shows that the new solution is in close agreement in both interfacial shear and normal stresses with those of literature. The solution methodology is general in nature and may be applicable to the analysis of other types of composite structures. In future other type of reinforcement can be considered as concrete columns or polymer matrix reinforced with nano-materials (Arani and Kolahchi 2016, Bilouei *et al*. 2016, Madani *et al*. 2016; Zamanian *et al*. 2017; Kolahchi *et al*. 2017a, Hajmohammad *et al*. 2017, Kolahchi and Cheraghbak 2017, Zarei *et al*. 2017, Hajmohammad *et al*. 2018a,b,c, Amnieh *et al*. 2018, Golabchi *et al*. 2018, Hosseini and Kolahchi 2018, Bakhadda *et al*. 2018). In addition, other theories and other types of materials (Bousahla *et al*. 2014, Belkorissat *et al*. 2015, Attia *et al*. 2015, Kolahchi *et al*. 2016, Kolahchi *et al*. 2016a,b, Beldjelili *et al*. 2016, Kolahchi 2017, Menasria *et al*. 2017, Kolahchi *et al*. 2017b,c, Fahsi *et al*. 2017, El-Haina *et al*. 2017, Bellifa *et al*. 2017, Fakhar and Kolahchi 2018, Fourn *et al*. 2018, Attia *et al*. 2018, Younsi *et al*. 2018, Benchohra *et al*. 2018, Belabed *et al*. 2018, Abualnour *et al*. 2018, Bourada *et al*. 2018, 2019, Bouhadra *et al*. 2018, Meksi *et al*. 2019) will be also employed to study this of problems.

References

Abualnour, M., Houari, M.S.A., Tounsi, A., Adda Bedia, E.A. and Mahmoud, S.R. (2018), "A novel quasi-3D trigonometric plate theory for free vibration analysis of advanced composite plates", *Compos. Struct*., **184**, 688-697.

Ahmed, A. (2014), "Post buckling analysis of sandwich beams with functionally graded faces using a consistent higher order theory", *Int. J. Civil Struct. Environ*., **4**(2), 59-64.

Akavci, S.S. and Tanrikulu, A.H. (2015), "Static and free vibration analysis of functionally graded plates based on a new quasi-3D and 2D shear deformation theories", *Compos. Part B*, **83**, 203-215.

Aldousari, S.M. (2017), "Bending analysis of different material distributions of functionally graded beam", *Appl. Phys. A: Mater. Sci. Proc*., **123**(4), 296.

Alfredsson, K.S. and Höberg, J.L. (2008), "A closed-form solution to statically indeterminate adhesive joint problems exemplified on ELS-specimens", *Int. J. Adhes. Adhesiv.*, **28**, 350-361.

Amnieh, H.B., Zamzam, M.S. and Kolahchi, R. (2018), "Dynamic analysis of non-homogeneous concrete blocks mixed by SiO2 nanoparticles subjected to blast load experimentally and theoretically", *Constr. Build. Mater.*, **174**, 633-644.

Antes, H. (2003), "Fundamental solution and integral equations for Timoshenko beams", *Comput. Struct*., **81**(6), 383-396.

Arani, A.J. and Kolahchi, R. (2016), "Buckling analysis of embedded concrete columns armed with carbon nanotubes", *Comput. Concrete*, **17**(5), 567-578.

Attia, A., Bousahla, A.A., Tounsi, A., Mahmoud, S.R. and Alwabli, A.S. (2018), "A refined four variable plate theory for thermoelastic analysis of FGM plates resting on variable elastic foundations", *Struct. Eng. Mech.*, **65**(4), 453-464.

Attia, A., Tounsi, A., Adda Bedia, E.A. and Mahmoud, S.R. (2015), "Free vibration analysis of functionally graded plates with temperature-dependent properties using various four variable refined plate theories", *Steel Compos. Struct*., **18**(1), 187-212.

Bakhadda, B., Bachir Bouiadjra, M., Bourada, F., Bousahla, A.A., Tounsi, A. and Mahmoud, S.R. (2018), "Dynamic and bending analysis of carbon nanotube-reinforced composite plates with elastic foundation", *Wind Struct.*, **27**(5), 311-324.

Belabed, Z., Bousahla, A.A., Houari, M.S.A., Tounsi, A. and Mahmoud, S.R. (2018), "A new 3-unknown hyperbolic shear deformation theory for vibration of functionally graded sandwich plate", *Earthq. Struct.*, **14**(2), 103-115.

Beldjelili, Y., Tounsi, A. and Mahmoud, S.R. (2016), "Hygro-thermo-mechanical bending of S-FGM plates resting on variable elastic foundations using a four-variable trigonometric plate theory", *Smart Struct. Syst.*, **18**(4), 755-786.

Belkorissat, I., Houari, M.S.A., Tounsi, A., Adda Bedia, E.A. and Mahmoud, S.R. (2015), "On vibration properties of functionally graded nano-plate using a new nonlocal refined four variable model", *Steel Compos. Struct*., **18**(4), 1063-1081.

Bellifa, H., Bakora, A., Tounsi, A., Bousahla, A.A. and Mahmoud, S.R. (2017), "An efficient and simple four variable refined plate theory for buckling analysis of functionally graded plates", *Steel Compos. Struct*., **25**(3), 257-270.

Benchohra, M., Driz, H., Bakora, A., Tounsi, A., Adda Bedia, E.A. and Mahmoud, S.R. (2018), "A new quasi-3D sinusoidal shear deformation theory for functionally graded plates", *Struct. Eng. Mech*., **65**(1), 19-31.

Bensaid, I. and Kerboua, B. (2017), "Interfacial stress analysis of functionally graded beams strengthened with a bonded hygrothermal aged composite plate", *Compos. Interf*., **24**(2), 149-169.

Bilouei, B.S., Kolahchi, R. and Bidgoli, M.R. (2016), "Buckling of concrete columns retrofitted with Nano-Fiber Reinforced Polymer (NFRP)", *Comput. Concrete*, **18**(5), 1053-1063.

Bouhadra, A., Tounsi, A., Bousahla, A.A., Benyoucef, S. and Mahmoud, S.R. (2018), "Improved HSDT accounting for effect of thickness stretching in advanced composite plates", *Struct. Eng. Mech*., **66**(1), 61-73.

Bourada, F., Amara, K., Bousahla, A.A., Tounsi, A. and Mahmoud, S.R. (2018), "A novel refined plate theory for stability analysis of hybrid and symmetric S-FGM plates", *Struct. Eng. Mech.*, **68**(6), 661-675.

Bourada, F., Bousahla, A.A., Bourada, M., Azzaz, A., Zinata, A. and Tounsi, A. (2019), "Dynamic investigation of porous functionally graded beam using a sinusoidal shear deformation theory", *Wind Struct.*, **28**(1), 19-30.

Bousahla, A.A., Houari, M.S.A., Tounsi, A. and Adda Bedia, E.A. (2014), "A novel higher order shear and normal deformation theory based on neutral surface position for bending analysis of advanced composite plates", *Int. J. Comput. Meth*., **11**(6), 1350082.

Chikh, A., Tounsi, A., Hebali, H. and Mahmoud, S.R. (2017), "Thermal buckling analysis of cross-ply laminated plates using a simplified HSDT", *Smart Struct. Syst.*, **19**(3), 289-297.

Cowper, G.R. (1966). "The shear coefficient in Timoshenko's beam theory", *J. Appl. Mech*., ASCE, **33**(2), 335-340.

Daouadji, T., Chedad, A. and Adim, B. (2016), "Interfacial stresses in RC beam bonded with a functionally graded material plate", *Struct. Eng. Mech.*, **60**(4), 693-705.

Daouadji, T.H. (2017), "Analytical and numerical modeling of interfacial stresses in beams bonded with a thin plate", *Adv. Comput. Des.*, **2**(1), 57-69.

Draiche, K., Tounsi, A. and Mahmoud, S.R. (2016), "A refined theory with stretching effect for the flexure analysis of laminated composite plates", *Geomech. Eng*., **11**(5), 671-690.

Edalati, M. and Fereidoon, I. (2012),"Interfacial stresses in RC beams strengthened by externally bonded FRP/steel plates with effects of shear deformation", *J. Compos. Constr.*, ASCE, **16**(1), 60-73.

El-Haina, F., Bakora, A., Bousahla, A.A., Tounsi, A. and Mahmoud, S.R. (2017), "A simple analytical approach for thermal buckling of thick functionally graded sandwich plates",

Struct. Eng. Mech., **63**(5), 585-595.

Etman, E.E. and Beeby, A.W. (2000), "Experimental programme and analytical study of bond stress distributions on a composite plate bonded to a reinforced concrete beam", *Cement Concrete Compos*., **22**(4), 281-91.

Fahsi, A., Tounsi, A., Hebali, H., Chikh, A., Adda Bedia, E.A. and Mahmoud, S.R. (2017), "A four variable refined nth-order shear deformation theory for mechanical and thermal buckling analysis of functionally graded plates", *Geomech. Eng.*, **13**(3), 385-410.

Fakhar, A. and Kolahchi, R. (2018), "Dynamic buckling of magnetorheological fluid integrated by visco-piezo-GPL reinforced plates", *Int. J. Mech. Sci.*, **144**, 788-799.

Fourn, H., Ait Atmane, H., Bourada, M., Bousahla, A.A., Tounsi, A. and Mahmoud, S.R. (2018), "A novel four variable refined plate theory for wave propagation in functionally graded material plates", *Steel Compos. Struct.*, **27**(1), 109-122.

Golabchi, H., Kolahchi, R. and Rabani Bidgoli, M. (2018), "Vibration and instability analysis of pipes reinforced by SiO2 nanoparticles considering agglomeration effects", *Comput. Concrete*, **21**(4), 431-440.

Guenaneche, B., Tounsi, A. and Adda Bedia, E.A. (2014), "Effect of shear deformation on interfacial stress analysis in plated beams under arbitrary loading", *Int. J. Adhes. Adhesiv.*, **48**, 1-13.

Guilbeau, L. (1930), "The history of the solution of the cubic equation", *Math. News Lett.*, **5**(4), 8-12. https://doi.10.2307/3027812.

Hajmohammad, M.H., Farrokhian, A. and Kolahchi, R. (2018a), "Smart control and vibration of viscoelastic actuator-multiphase nanocomposite conical shells-sensor considering hygrothermal load based on layerwise theory", *Aerosp. Sci. Technol.*, **78**, 260-270.

Hajmohammad, M.H., Kolahchi, R., Zarei, M.S. and Maleki, M. (2018d), "Earthquake induced dynamic deflection of submerged viscoelastic cylindrical shell reinforced by agglomerated CNTs considering thermal and moisture effects", *Compos. Struct.*, **187**, 498-508.

Hajmohammad, M.H., Maleki, M. and Kolahchi, R. (2018b), "Seismic response of underwater concrete pipes conveying fluid covered with nano-fiber reinforced polymer layer", *Soil Dyn. Earthq. Eng.*, **110**, 18-27.

Hajmohammad, M.H., Zarei, M.S., Nouri, A. and Kolahchi, R. (2017), "Dynamic buckling of sensor/functionally graded-carbon nanotube-reinforced laminated plates/actuator based on sinusoidal-visco-piezoelasticity theories", *J. Sandw. Struct. Mater.*, 1099636217720373.

Hollaway, L.C. and Leeming, M.B. (1999), *Strengthening of Reinforced Concrete Structures using Externally-Bonded FRP Composites in Structural and Civil Engineering. Cambridge*, Woodhead Publishing Ltd., UK

Hosseini, H. and Kolahchi, R. (2018), "Seismic response of functionally graded-carbon nanotubes-reinforced submerged viscoelastic cylindrical shell in hygrothermal environment", *Physica E: Lowdimens. Syst. Nanostr.*, **102**, 101-109.

Kaci, A., Houari, M.S.A., Bousahla, A.A., Tounsi, A. and Mahmoud, S.R. (2018), "Post-buckling analysis of shear-deformable composite beams using a novel simple two-unknown beam theory", *Struct. Eng. Mech.*, **65**(5), 621-631.

Kolahchi, R. (2017), "A comparative study on the bending, vibration and buckling of viscoelastic sandwich nano-plates based on different nonlocal theories using DC, HDQ and DQ methods", *Aerosp. Sci. Technol.*, **66**, 235-248.

Kolahchi, R. and Cheraghbak, A. (2017), "Agglomeration effects on the dynamic buckling of viscoelastic microplates reinforced with SWCNTs using Bolotin method", *Nonlin. Dyn.*, **90**, 479-492.

Kolahchi, R. and Moniri Bidgoli, A.M. (2016), "Size-dependent sinusoidal beam model for dynamic instability of single-walled carbon nanotubes", *Appl. Math. Mech.*, **37**(2), 265-274.

Kolahchi, R., Hosseini, H. and Esmailpour, M. (2016a), "Differential cubature and quadrature-Bolotin methods for dynamic stability of embedded piezoelectric nanoplates based on visco-nonlocal-piezoelasticity theories", *Compos. Struct.*, **157**, 174-186.

Kolahchi, R., Keshtegar, B. and Fakhar, M.H. (2017c), "Optimization of dynamic buckling for sandwich nanocomposite plates with sensor and actuator layer based on sinusoidal-visco-piezoelasticity theories using Grey Wolf algorithm", *J. Sandw. Struct. Mater.*, 1099636217731071. https://doi.org/10.1177/1099636217731071.

Kolahchi, R., Safari, M. and Esmailpour, M. (2016b), "Dynamic stability analysis of temperature-dependent functionally graded CNT-reinforced visco-plates resting on orthotropic elastomeric medium", *Compos. Struct.*, **150**, 255-265.

Kolahchi, R., Zarei, M.S., Hajmohammad, M.H. and Nouri, A. (2017a), "Wave propagation of embedded viscoelastic FG-CNT-reinforced sandwich plates integrated with sensor and actuator based on refined zigzag theory", *Int. J. Mech. Sci.*, **130**, 534-545.

Kolahchi, R., Zarei, M.S., Hajmohammad, M.H. and Oskouei, A.N. (2017b), "Visco-nonlocal-refined Zigzag theories for dynamic buckling of laminated nanoplates using differential cubature-Bolotin methods", *Thin Wall. Struct.*, **113**, 162-169.

Kreja, I. (2011), "A literature review on computational models for laminated composite and sandwich panels", *Cent. Eur. J. Eng.*, **1**(1), 59-80.

Kurtz, S., Balaguru, P. and Helm, J. (2008), "Experimental study of interfacial shear stresses in FRP-strengthened RC beams", *J. Compos. Constr.*, **12**(3), 312-322. https://doi.org/10.1061/(ASCE)1090-0268(2008)12:3(312).

Maalej, M. and Bian, Y. (2001), "Interfacial shear stress concentration in FRP strengthened beams", *Compos. Struct.*, **54**(4), 417-426.

Maalej, M. and Leong, K.S. (2005), "Effect of beam size and FRP thickness on interfacial shear stress concentration and failure mode of FRP strengthened beams", *Compos. Sci. Technol.*, **65**(7-8), 1148-1158.

Madani, H., Hosseini, H. and Shokravi, M. (2016), "Differential cubature method for vibration analysis of embedded FG-CNT-reinforced piezoelectric cylindrical shells subjected to uniform and non-uniform temperature distributions", *Steel Compos. Struct.*, **22**(4), 889-913.

Mahi, A., Adda Bedia, E.A. and Tounsi, A. (2015), "A new hyperbolic shear deformation theory for bending and free vibration analysis of isotropic, functionally graded, sandwich and laminated composite plates", *Appl. Math. Model.*, **39**(9), 2489-2508.

Malek, A.M., Saadatmanesh, H. and Ehsani, M.R. (1998), "Prediction of failure load of R/C beams strengthened with FRP plate due to stress concentration at the plate end", *ACI Struct. J.*, **95**(1), 142-52.

Meksi, R., Benyoucef, S., Mahmoudi, A., Tounsi, A., Adda Bedia, E.A. and Mahmoud, S.R. (2019), "An analytical solution for bending, buckling and vibration responses of FGM sandwich plates", *J. Sandw . Struct. Mater.*, **21**(2), 727-757.

Menasria, A., Bouhadra, A., Tounsi, A., Bousahla, A.A. and Mahmoud, S.R. (2017), "A new and simple HSDT for thermal stability analysis of FG sandwich plates", *Steel Compos. Struct.*, **25**(2), 157-175.

Narayanamurthy, V., Chen, J.F. and Cairns, J. (2016), "Improved model for interfacial stresses accounting for the effect of shear deformation in plated beams", *Int. J. Adhes. Adhesiv.*, **64**, 33-47.

Panjehpour, M., Ali, A.A.A. and Aznieta, F.N. (2014a), "Energy

absorption of reinforced concrete deep beams strengthened with CFRP sheet", *Steel Compos. Struct.*, **16**(5), 481-489.
Panjehpour, M., Ali, A.A.A., Voo, Y.L. and Aznieta, F.N. (2014b), "Effective compressive strength of strut in CFRP-strengthened reinforced concrete deep beams following ACI 318-11", *Comput. Concrete*, **13**(1), 135-165.
Rabahi, A., Adim, B., Chargui, S. and Hassaine Daouadji, T. (2015), "Interfacial Stresses in FRP-plated RC Beams: Effect of Adherend Shear Deformations", *Multiphys. Model. Simul. Syst. Des. Monit.*, **2**, 317-326.
Rabinovitch, O. and Frostig, Y. (2000), "Closed-form high-order analysis of RC beams strengthened with FRP strips", *J. Compos. Constr.*, ASCE, **4**(2), 65-74.
Roberts, T.M. (1989), "Approximate analysis of shear and normal stress concentrations in the adhesive layer of plated RC beams", *Struct. Eng.*, **67**(12), 229-233.
Roberts, T.M. and Haji-Kazemi, H. (1989), "Theoretical study of the behavior of reinforced concrete beams strengthened by externally bonded steel plates", *Proc. Inst. Civil Eng.*, **87**(2), 39-55.
Sahoo, S.S., Panda, S.K. and Mahapatra, T.R. (2017), "Static, free vibration and transient response of laminated composite curved shallow panel-an experimental approach", *Eur. J. Mech., A/Solid.*, **59**, 95-113.
Shen, H.S., Teng, J.G. and Yang, J. (2001), "Interfacial stresses in beams and slabs bonded with thin plate", *J. Eng. Mech*., ASCE, **127**(4), 399-406.
Smith, S.T. and Teng, J.G. (2001), "Interfacial stresses in plated beams", *Eng. Struct*., **23**(7), 857-871.
Stafford, S.B. and Coull, A. (1991), *Tall Building Structures: Analysis and Design*, Wiley, New York.
Taljsten, B. (1997), "Strengthening of beams by plate bonding", *J. Mater. Civil Eng*., ASCE, **9**(4), 206-212.
Teng, J.G., Cheng, J.F., Smith, S.T. and Lam, L. (2002a), *FRP-Strengthened RC Structures*, West Sussex, Wiley.
Teng, J.G., Cheng, J.F., Smith, S.T. and Lam, L. (2003), "Behavior and strength of FRP-strengthened RC structures: a state-of-the-art review", *Proc. Inst. Civil Eng., Struct. Build.*, **156**(1), 51-62.
Teng, J.G., Zhang, J.W. and Smith, S.T. (2002b), "Interfacial stresses in reinforced concrete beams bonded with a soffit plate: a finite element study", *Constr. Build. Mater*., **16**(1), 1-14.
Timoshenko, S. and Gere, J.M. (1984), *Mechanics of Materials*, Van Nostrand Reinhold Co.
Tounsi A. (2006), "Improved theoretical solution for interfacial stresses in concrete beams strengthened with FRP plate", *Int. J. Solid. Struct*., **43**, 4154-74.
Tounsi, A., Hassaine, D.T., Benyoucef, S. and Adda, B.E.A. (2009), "Interfacial stresses in FRP-plated RC beams: Effect of adherend shear deformations", *Int. J. Adhes. Adhesiv*., **29**(4), 343-351.
Tsai, M.Y., Oplinger, D.W. and Morton, J. (1998), "Improved theoretical solutions for adhesive lap joints", *Int. J. Solid. Struct*., **35**(12), 1163-1185.
Vilnay, O. (1988), "The analysis of reinforced concrete beams strengthened by epoxy bonded steel plates", *Int. J. Cement Compos. Lightw. Concrete*, **10**(2), 73-78.
Wu, Z.S., Yuan, H., Kojima, Y. and Ahmed, E. (2005), "Experimental and analytical studies on peeling and spalling resistance of unidirectional FRP sheets bonded to concrete", *Compos. Sci. Technol*., **65**(7-8), 1088-1097.
Yang, J. and Wu, Y.F. (2007), "Interfacial stresses of FRP strengthened concrete beams: Effect of shear deformation", *Compos. Struct*., **80**(3), 343-351.
Yang, Q.S., Peng, X.R. and Kwan, A.K.H. (2004), "Finite element analysis of interfacial stresses in FRP-RC hybrid beams", *Mech. Res. Commun*., **31**(3), 331-340.
Ye, J.Q. (2001), "Interfacial shear stress transfer of RC beams strengthened by bonded composite plates", *Cement Concrete Compos*., **23**(4-5), 411-417.
Younsi, A., Tounsi, A., Zaoui, F.Z., Bousahla, A.A. and Mahmoud, S.R. (2018), "Novel quasi-3D and 2D shear deformation theories for bending and free vibration analysis of FGM plates", *Geomech. Eng.*, **14**(6), 519-532.
Zamanian, M., Kolahchi, R. and Bidgoli, M.R. (2017), "Agglomeration effects on the buckling behaviour of embedded concrete columns reinforced with SiO2 nano-particles", *Wind Struct*., **24**(1), 43-57.
Zarei, M.S., Kolahchi, R., Hajmohammad, M.H. and Maleki, M. (2017), "Seismic response of underwater fluid-conveying concrete pipes reinforced with SiO2 nanoparticles and fiber reinforced polymer (FRP) layer", *Soil Dyn. Earthq. Eng*., **103**, 76-85.
Zine, A., Tounsi, A., Draiche, K., Sekkal, M. and Mahmoud, S.R. (2018), "A novel higher-order shear deformation theory for bending and free vibration analysis of isotropic and multilayered plates and shells", *Steel Compos. Struct.*, **26**(2), 125-137.

CC